Systematic Control of Experimental Inconsistency in Combinatorial Materials Science

Asish Kumar Sharma,[†] Chandramouli Kulshreshtha,[†] Keemin Sohn,[‡] and Kee-Sun Sohn*,[†]

Department of Materials Science and Metallurgical Engineering, Sunchon National University, Chonnam 540-742, Korea, and Department of Urban Infrastructure, Seoul Development Institute, Seoul 135-071, Korea

Received July 4, 2008

We developed a method to systematically control experimental inconsistency, which is one of the most troublesome and difficult problems in high-throughput combinatorial experiments. The topic of experimental inconsistency is never addressed, even though all scientists in the field of combinatorial materials science face this very serious problem. Experimental inconsistency and material property were selected as dual objective functions that were simultaneously optimized. Specifically, in an attempt to search for promising phosphors with high reproducibility, photoluminescence (PL) intensity was maximized, and experimental inconsistency was minimized by employing a multiobjective evolutionary optimization-assisted combinatorial materials search (MOEO combinatorial material search) strategy. A tetravalent manganese-doped alkali earth germanium/titanium oxide system was used as a model system to be screened using MOEO combinatorial materials search. As a result of MOEO reiteration, we identified a halide-detached deep red phosphor with improved PL intensity and reliable reproducibility.

1. Introduction

Combinatorial materials science based on high-throughput experimentation (HTE) has evolved considerably in recent decades and its applications now include a variety of materials.[1−16] Recently, combinatorial materials science has shifted from "simple-mixing" to "smart-mixing" strategies. A smart-mixing strategy that has attracted considerable interest is genetic algorithm-assisted combinatorial materials search (GACMS).[21−28] The use of genetic algorithms is one of the most efficient stochastic optimization strategies employed to solve multidimensional problems.[17−20] In this regard, the combination of GA and HTE results in a highly efficient system that enables the development of new materials and catalysts.[21−30] For instance, we have identified some promising luminescent multicompositional inorganic compounds using GACMS.[29,30]

No matter which strategy is adopted for HTE-based optimization processes, minimization of experimental error is critical. Error-free experimental processes are also very important in GACMS because evaluation of an unknown objective (either fitness or cost) function is performed by actual synthesis and subsequent characterization. Experimental evaluation of an unknown objective function always gives rise to experimental error or inconsistency. Thus, in our previous reports, we dealt with experimental inconsistency in two ways.[29,30] We reproduced elitized members and, subsequently, regarded them as indicators of inconsistency. Alternatively, we conducted confirmative, auxiliary experiments, wherein a replicate of each library was produced, such that differences between the original and replicate libraries were closely monitored. These methods yielded a stopping criterion indicating the point at which the process should be aborted. However, we failed to systematically control experimental inconsistency because of a misunderstanding of the problem. As a result, many experiments, consuming enormous effort, time, and monetary resources, proved futile because of inconsistency during the GACMS process. In our experience, failed experiments occur more frequently than do successful experimental processes that lead to publications.[29,30]

Experimental inconsistency may be caused by external factors, such as imperfect experimental apparatuses, environmental effects, or investigator error. However, extrinsic error can be reduced to an acceptable level by use of sophisticated methods. In addition, we have characterized extrinsic error to minimize its influence during the current stage of development. What interests us most is not the controllable extrinsic error, but the intrinsic error that cannot be easily controlled because its origin is unknown. In contrast to the readily identifiable causes of extrinsic error, the most problematic and troublesome intrinsic error originates from uncontrollable solution behaviors. Because the precursor solutions used in our experiments contained at least six cations, it was nearly impossible to discern either the behavior of each cation or the more complicated interactions among cations in the mixture during the GACMS process. The ensuing solid-state syntheses should also have intrinsic inconsistency. The presence of inconsistency in the solid-

* To whom correspondence should be addressed. E-mail: kssohn@sunchon.ac.kr.
[†] Sunchon National University.
[‡] Seoul Development Institute.

10.1021/cc800116q CCC: $40.75
Published on Web 12/05/2008

state synthesis is inevitable as argued by Jansen,[31] wherein the inherent unpredictability of synthesis in the solid state was discussed. Thus, it is reasonable to hypothesize that experimental inconsistency is strongly dependent on the composition of the precursor solution and to therefore treat experimental inconsistency as a function of composition. Therefore, the experimental inconsistency can be considered an unknown objective function that is minimized during the GACMS process. One of possible approaches to simultaneously minimize experimental inconsistency and optimize material properties is a multiobjective evolutionary optimization (MOEO). Therefore, we used an MOEO-assisted combinatorial materials search to identify promising phosphors. Specifically, we set both the luminescent intensity and the inconsistency index, which is the relative difference in photoluminescence (PL) intensity between two compounds with identical compositions from separately prepared libraries, as objective functions in our MOEO-assisted combinatorial material search process. As expected, MOEO-assisted combinatorial material search allowed for simultaneous maximization of PL intensity and minimization of the inconsistency index.

2. Multiobjective Evolutionary Optimization (MOEO)

The genetic algorithm (GA) is one of the most widely used evolutionary optimizations. GA is a stochastic global search method that mimics natural biological evolution. A GA operates on a population of potential solutions, applying Darwin's principle of survival of the fittest. GAs use techniques such as inheritance (elitism), mutation, selection, and crossover. GAs make populations evolve, that is, they make individuals that are better suited to their environment survive. The evolution usually starts from a population of randomly generated individuals (randomly generated phosphor composition in the present case). In the first generation, the fitness (one of the phosphor properties in the present case, e.g., luminescent intensity) of every individual in the population is evaluated; multiple individuals are stochastically selected from the current population based on their fitness (e.g., roulette-wheel or tournament selection) and modified by crossover and mutation to form a new population. The new population is then used in the next iteration of the algorithm. The string of decision parameters (composition of phosphors in the present case) represented in binary codes is regarded as a chromosome and each parameter can be thought of as a gene.[17−19]

Multiobjective optimization problems (MOP) consist of multidimensional decision vectors and multidimensional objective vectors. In the present case, we have six decision parameters and two objective functions.

$$\mathbf{y} = \{f_1(\mathbf{x}) : \text{Maximize}, f_2(\mathbf{x}) : \text{Minimize}\} \in Y$$
$$\text{where } \mathbf{x} = \{x_1, x_1, x_3, ..., x_6\} \in X$$

X stands for a decision parameter space, $\mathbf{x}$ is a decision parameter vector, and x_{1-6} are decision parameters. Y stands for an objective function space, $\mathbf{y}$ is an objective function vector, and $f_1(\mathbf{x})$ and $f_2(\mathbf{x})$ are objective functions. Namely, the first objective function, $f_1(\mathbf{x})$, which is maximized, is luminescent intensity. The second objective function, $f_2(\mathbf{x})$, which is minimized, is the inconsistency index. The phosphor composition, that is, the mole fractions of Ca, Ba, Mg, Ge, Ti, and Mn, is represented by x_{1-6}. An important issue for MOPs is Pareto optimality,[18,32−39] which determines the relative dominance of the luminescent intensity and inconsistency index.

The basic algorithm of GAs has been extended to solve problems with multiple objectives. The goal of the multiobjective optimization is to find a set of nondominated solutions (ideally with a good spread) by the assist of genetic algorithm. For this sake, Fonseca Fleming[34] proposed the multi-objective genetic algorithm (MOGA), and Srinivas and Deb[36] proposed the nondominated sorting genetic algorithm (NSGA). Both approaches consist of a similar scheme in which the rank of a certain individual is determined. Accordingly, the main concept of MOGA and NSGA is the same in principle. They slightly differ in the way of deciding ranks and assigning fitness values. We adopted NSGA[36−38] in the present investigation. NSGA has been described in detail in literature,[32−39] NSGA is based on several layers of classifications of the individuals. Before selection is performed (roulette wheel selection was used), the population is ranked on the basis of domination (using Pareto ranking): all nondominated individuals are classified into one category with a dummy fitness value. To maintain the diversity of the population, these classified individuals are shared with their dummy fitness values. Then this group of classified individuals is removed from the population, and another layer of nondominated individuals is considered (i.e., the remainder of the population is reclassified). The process continues until all individuals in the population are classified. Since individuals in the first front have the maximum fitness value, they always get more copies than the rest of the population. This allows us to search for nondominated regions (Pareto fronts) and results in convergence of the population toward such regions. The algorithm is similar to a simple GA, except for the classification of nondominated fronts and the sharing operation. Fitness sharing, so-called niche sharing or niching, helps to distribute the population over this region.[18,35−39]

Fitness sharing disperses densely populated regions. It lowers each population element's fitness by an amount nearly equal to the number of similar individuals in the population. Typically, the shared fitness, fi', of an individual with fitness f_i is simply $fi' = f_i/m_i$, where m_i is the niche count which measures the approximate number of individuals with whom the fitness f_i is shared. The niche count is calculated by summing a sharing function over all members of the current Pareto front.

$$m_i = \sum_j^N \text{sh}(d_{ij})$$

$$\text{sh}(d_{ij}) = \begin{cases} 1 - \left(\dfrac{d_{ij}}{\sigma_{\text{shared}}}\right) & \text{if } d_{ij} < \sigma_{\text{shared}} \\ 0 & \text{otherwise} \end{cases}, \qquad \sigma_{\text{shared}} = \frac{\sqrt{k}}{\sqrt{p}}$$

Where N denotes the population size and d_{ij} represents the distance between individuals. Thence, the sharing function $\text{sh}(d_{ij})$ measures the similarity level between two population elements. σ_{share} denotes the threshold of dissimilarity (also

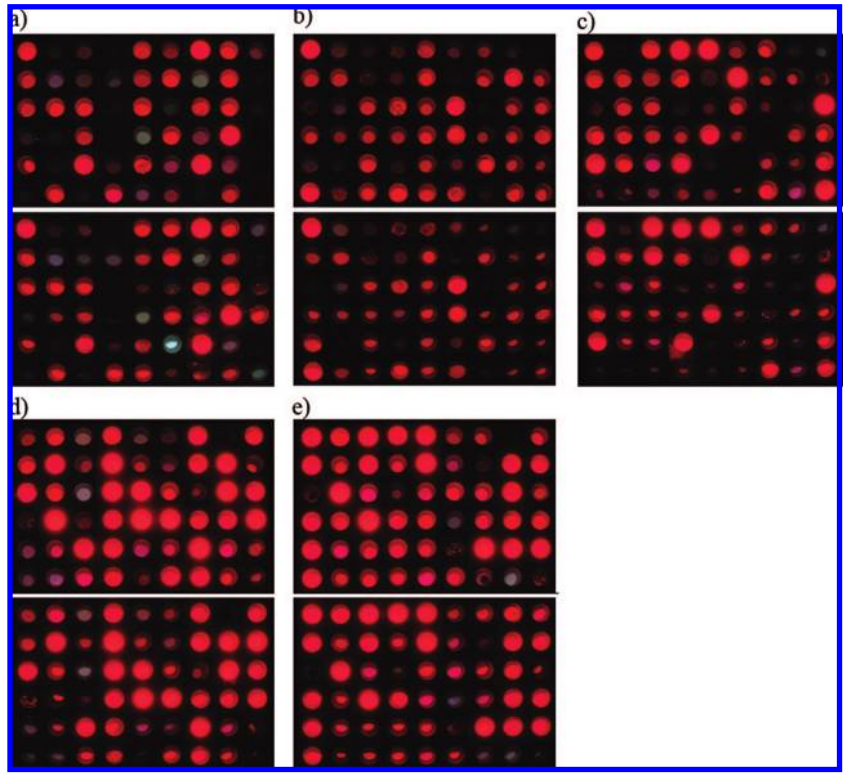

Figure 1. Photographs of each generation and replicate. The first row of a, b, c, d, and e shows of generations 1−5, and the second row shows the replicates under excitation at 254 nm, respectively. The generation number increases from left to right. Direct comparison among these photographs is appropriate, as all the photographs were taken under the same conditions. Nevertheless, improvements in both PL intensity and consistency are clearly evident.

the distance cutoff or the niche radius), where k is the number of dimensions and p is the population size of the current Pareto front. Finally, the shared fitness value of each individual is calculated by dividing its dummy fitness value by its niche count. The completion of the fitness sharing leads to GA routines such as roulette-wheel selection, crossover, and mutation. Details about this general GA implementation after the fitness sharing processes are well described in our previous works.[29,40]

3. Experimental Procedures

The $MnO-CaO-BaO-MgO-GeO_2-TiO_2$ six-dimensional library compositions were prepared and screened using the solution-dependent combinatorial library method based on a high-throughput screening technique. All chemicals such as manganese nitrate hydrous ($Mn(NO_3)_2 \cdot xH_2O$), calcium nitrate hydrous ($Ca(NO_3)_2 \cdot xH_2O$), barium nitrate ($Ba(NO_3)_2$), magnesium nitrate hydrous ($Mg(NO_3)_2 \cdot 6H_2O$)), 3,3′-(1,3-dioxo-1,3-digermoxanediyl)bispropionic acid ($C_6H_{10}Ge_2O_7$), and titanium(IV)(triethanolaminato)-isopropoxide (80 wt % solution in propanol) ($C_9H_{19}NO_4Ti$) were prepared in deionized water. Organic precursors, such as 3,3′-(1,3-dioxo-1,3-digermoxanediyl)bispropionic acid, commonly known as Ge-132, and titanium(IV)(triethanolaminato)-isopropoxide (80 wt % solution in propanol), underwent special treatment. Ge-132, which is insoluble in water at high concentrations, was prepared in warm water at 30 °C. The Ti(IV) solution, which precipitates with other solutions at high concentrations, was prepared in a solution of citric acid (0.1 M). Therefore, the concentrations of Ge-132 and Ti (IV) were less than the concentrations of the other solutions. The total volume of one library was increased to 14 mL to obtain an adequate amount of compound. The calculated volume of each solution for every generation was then pipetted into a 16 × 150 mm test tube, according to the composition table. For each generation, 54 solutions were prepared. The solutions were then dried at 85−130 °C for 96 h in an oven. The samples were heated in a box furnace in a stepwise manner, that is, 300 °C/3 h, to prevent rapid evaporation. Dried samples were gently pulverized and heated again at 600 °C/3 h. The dried samples were pulverized and transferred to a specially designed alumina "combichem"container,[29] in which they were heated at 1150 °C for 20 h in an oxidizing atmosphere so as to keep manganese in the Mn^{4+} state. This process was repeated once for each generation to produce a replicate that was used to estimate the inconsistency index.

The emission spectrum was measured at an excitation wavelength of 254 nm in continuous wave (CW) mode at wavelengths ranging from 450 to 800 nm at room temperature using a spectrophotometer (Professional Scientific Instrument Ltd. Co., PS-PLU-X1420) equipped with a deuterium lamp. The excitation spectrum was measured at a probing wavelength of 661 nm over a range of 220−500 nm. X-ray powder diffraction patterns were measured using Cu Kα radiation at 40 kV and 30 mA (Panalytical X'pert Pro Pw 3060 MRD).

4. Results and Discussions

A tetravalent manganese-doped alkali earth germanium/titanium oxide system ($MnO-CaO-BaO-MgO-GeO_2-TiO_2$ six-dimensional compositions), which emits a deep red

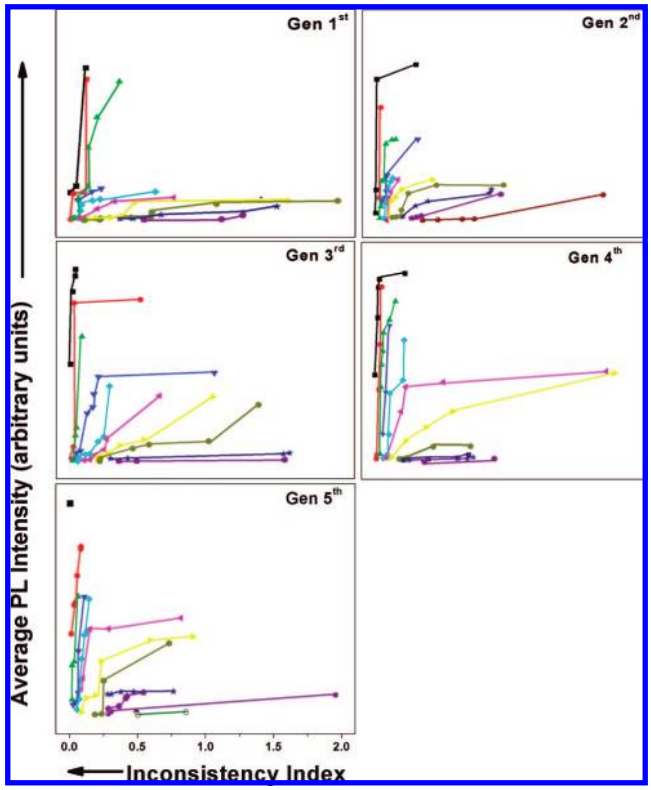

Figure 2. Pareto surface for each generation. A Pareto surface for each generation by plotting average PL intensity vs the inconsistency index value. Each Pareto surface-front is shown in a unique color, for example, the first and second Pareto fronts are shown in black and red, respectively, and data points are also shown. (The composition table for all members, exact average intensity, and inconsistency index values are presented in the Supporting Information.)

color, was screened by NSGA-assisted combinatorial material search using PL intensity and the inconsistency index as objective functions. PL intensity, which was maximized, was the first objective function. The inconsistency index, which was minimized, was our second objective function. The compositions of library members were treated as decision parameters. The variance in measured PL intensity for each composition should provide a superior indicator of experimental inconsistency. However, it should be noted that generation of a large amount of statistical data is impractical, even though HTE techniques are used. Therefore, the inconsistency index was determined from only two separate libraries. For this reason, we termed this measure the inconsistency index, rather than variance. The inconsistency index appears to be an adequate indicator of experimental inconsistency.

Figure 1 and Figure 2 show five libraries (generations) photographed under 254-nm excitation and graphs exhibiting Pareto sorting for each generation. As NSGA was reiterated to the fifth generation, both the PL intensity and experimental inconsistency improved, resulting in identification of a phosphor with improved PL intensity and high reproducibility. Figure 1 clearly shows that the number of promising members (bright-red-light-emitting members) increased in the later generations. For example, in the first generation, approximately 27 out of 54 members were unacceptable, exhibiting either no light emission or nonred-light emission; however, in the fifth generation, only 10 of 54 members were unacceptable. The non-red-light emission originates from divalent-manganese-activated samples that we intended to eliminate. The presence of the undesirable divalent manganese samples is a nearly unavoidable complication, which is not easy to control experimentally because the valence state changes with the composition, even under constant processing conditions. The presence of divalent manganese increased the experimental inconsistency. Relative to the first generation, which was randomly defined, later generations that underwent evolutionary improvement exhibited significant improvements in the inconsistency index. While the photographs in Figure 1 allow only rough estimation of PL intensity and the inconsistency index, Figure 2 shows a Pareto front for each generation.

By coincidence, we found only one sample in the first Pareto front of the fifth generation. The performance of this sample was outstanding in terms of both PL intensity and experimental consistency. Specifically, the PL intensity was at the maximum, and the inconsistency index was almost zero. This implies that the method gave the same result on two separate occasions, thereby suggesting highly reliable reproducibility of sample preparation. This sample, hereafter referred to as sample S, was reproduced several more times to achieve complete reproducibility. Subsequently, reproducibility was validated.

After demonstrating the efficacy of our NSGA-assisted combinatorial material search, we next investigated the effects of material composition. First of all, it should be noted that the six-dimensional composition system ($MnO-CaO-BaO-MgO-GeO_2-TiO_2$) that we screened in the present investigation was very similar to our previous system ($MnO-CaO-SrO-BaO-MgO-GeO_2$) that implemented only by single objective GA, as recently reported.[40] Because our primary objective was to confirm the validity and practicality of our NSGA-assisted combinatorial material search approach that used both PL-intensity maximization and experimental-inconsistency minimization, we needed a model system for which the optimal point could be easily predicted based on our previous report. Therefore, we adopted a composition system similar to that used in our previous report.

The only difference between the present and previous systems was the inclusion of TiO_2 and the exclusion of SrO. In spite of these differences, the composition of sample S was similar to that of the final samples that we fully optimized in the previous report.[40] Thus, in both studies, the optimization processes occurred in the same direction and ultimately gave identical optimal structures, which was revealed to be $Mg_{14}Ge_5O_{24}:Mn^{4+}$ with a small amount of Ca-doping. In our previous report, we did not focus on the role of Ca-doping,[40] even though it was clear that Ca-doping was partly responsible for the enhancement of luminescence. The results of the present study confirm the positive effects of Ca-doping on luminescence.

Figure 3a shows the emission and excitation spectra of sample S. The narrow bands constituting the emission spectra originated from Jahn−Teller splitting of $^4F_2 \rightarrow {}^4A_2$ transitions of Mn^{4+} (d^3) ions.[41] The XRD pattern of sample S is

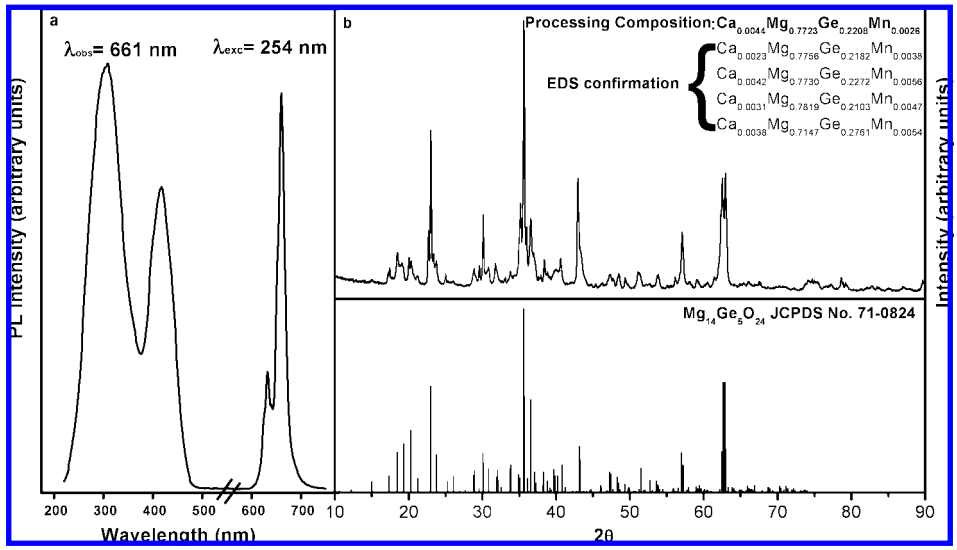

Figure 3. Excitation, emission, and XRD pattern of best sample S. (a, left panel) Excitation (left spectrum) and emission spectra (right spectrum) obtained for sample S, (b, right panels) XRD analysis of sample S (top), and a standard (bottom). The inset in the XRD graph of Sample S shows the results from the elemental analysis using energy dispersive spectroscopy (EDS) along with the real composition (top).

presented in Figure 3b, together with a standard from the Joint Committee on Powder Diffraction Standards (JCPDS). The inset in Figure 3b exhibits the composition table exhibiting the processing composition of sample S, along with the results from the elemental analysis using energy dispersive spectroscopy (EDS). The EDS analysis is powerful for a rough measure of composition but is not 100% correct. However, the coincidence was detected between the XRD and the EDS result, within an acceptable experimental error range, reflecting that the exact composition of sample S is Ca-co-doped $Mg_{14}Ge_5O_{24}:Mn^{4+}$. The processing composition of sample S is slightly different from the actual stoichiometry, $Mg_{14}Ge_5O_{24}$. For instance, the (Ca + Mg + Mn)/Ge ratio of sample S in terms of processing composition was approximately 3.5, which was slightly higher than the Mg/Ge ratio of $Mg_{14}Ge_5O_{24}$. It is customary to be faced with such an excessive alkali earth elements in liquid solution-based syntheses.[30,40] It is manifest that if we had adopted the exact stoichiometry ($Mg_{14}Ge_5O_{24}$) at the initial composition design stage of the synthesis process, we would never have gotten to it. In this regard, the excessive amount of alkali earth elements is necessary to achieve the $Mg_{14}Ge_5O_{24}$ stoichiometry. The processing composition is based on trial-error strategies in general solution-based syntheses. Thus, this cumbersome process is time-consuming and expensive. However, it should be noted that the NSGA-assisted combinatorial material search process guided us to do this automatically without any high-cost endeavors nor in-depth consideration. More importantly, the NSGA-assisted combinatorial material search process enabled us to complete these procedures with high precision and reliable reproducibility in a very short time frame.

Sample S was codoped with very small amounts of calcium. It is noteworthy that evolution of the process resulted in elimination of the Ti and Ba codopants. Sample S consisted mostly of $Mg_{14}Ge_5O_{24}$. It should be noted that the structures of $Mg_{14}Ge_5O_{24}$ compounds are well-known,[42] and several similar compounds that incorporate divalent manganese are red phosphors.[43−47] However, tetravalent manganese-activated $Mg_{14}Ge_5O_{24}$ systems have never been considered as phosphors. Although the emission of $Mg_{14}Ge_5O_{24}:Mn^{4+}$ phosphors is less efficient than that of well-known halide-involved magnesium germanate systems, such as $Mg_2Ge_8O_{11}F_2:Mn^{4+}$, the color chromaticity of $Mg_{14}Ge_5O_{24}:Mn^{4+}$ phosphors (CIE $x = 0.71$, CIE $y = 0.29$) is as good as that of the $Mg_2Ge_8O_{11}F_2:Mn^{4+}$ phosphor. The Ca-co-doped $Mg_{14}Ge_5O_{24}:Mn^{4+}$ phosphor, which was identified using NSGA-assisted combinatorial material search, has potential as a deep-red phosphor for cold cathode fluorescent lamps (CCFL) in liquid crystal displays (LCD). Thus, the primary goal of this study, development of a halide-detached deep-red phosphor based on Mn^{4+} activated oxide system, was achieved. It should be noted that the inclusion of halides into the phosphor host structure is generally disadvantageous in both use and preparation.

5. Conclusion

In summary, we developed a method for the systematic control of experimental inconsistency, which is one of the most troublesome and difficult problems in high-throughput combinatorial experiments. The topic of experimental inconsistency has previously not been addressed, even though it is a very serious problem faced by all scientists in the field of combinatorial materials science. NSGA-assisted combinatorial material search was employed to screen tetravalent manganese-doped alkali earth germanium/titanium oxide systems to reproducibly identify deep-red phosphors. NSGA-assisted combinatorial material search effectively facilitated the search process and made it possible to control and, eventually, minimize experimental inconsistency in a systematic manner. Previously, experimental inconsistency was not accounted for systematically. Thus, we suggest that experimental inconsistency should be addressed in all types of HTE processes. Furthermore, NSGA-assisted combina-

torial material search is currently one of the most promising strategies to deal with experimental inconsistency. NSGA-assisted combinatorial material search process is highly recommended to those who encounter experimental inconsistency during the development of solution-synthesis-based combinatorial libraries.

In the model system that we used to determine the efficacy of our NSGA-assisted combinatorial material search method, five generations, including 270 phosphor samples and their replicates, were produced, and we finally identified the phosphor with maximal PL intensity and minimal experimental inconsistency, sample S. Sample S showed promising luminescence and was reliably reproduced. Phase identification of sample S revealed that the main phase of sample S was $Mg_{14}Ge_5O_{24}:Mn^{4+}$ and that a small amount of calcium-doping enhanced PL intensity. The promising luminescence and high reproducibility of sample S are advantageous to mass production, should the compound be commercialized. Consequently, this deep-red-emitting oxide phosphor may be useful in flat panel displays, white-light-emitting diodes, or even in Si-based solar cell applications, as a down-converting phosphor.

Acknowledgment. This work was supported by the Ministry of Commerce, Industry, and Energy (MOCIE) through the fostering project of Regional Innovation Center (RIC).

Supporting Information Available. The composition table for all members (each generation), inconsistency index values, and exact average intensity. This material is available free of charge via the Internet at http://pubs.acs.org.

References and Notes

(1) Xiang, X.-D.; Sun, X.; Briceno, G.; Lou, Y.; Wang, K.-A.; Chang, H.; Wallace-Freedman, W. G.; Chen, S.-W.; Schultz, P. G. *Science* **1995**, *268*, 1738.
(2) Sun, X.-D.; Gao, C.; Wang, J.; Xiang, X.-D. *Appl. Phys. Let.* **1997**, *70*, 3353.
(3) Sun, X.-D; Wang, K.-A.; Yoo, Y.; Wallace-Freedman, W. G.; Gao, C.; Xiang, X.-D; Schultz, P. G. *Adv. Mater.* **1997**, *9*, 1046.
(4) Danielson, E.; Golden, J. H.; McFarland, E. W.; Reaves, C. M.; Weinberg, W. H.; Wu, X. D. *Nature* **1997**, *389*, 944.
(5) Danielson, E.; Devenney, M.; Giaquinta, D. M.; Golden, J. H.; Haushalter, R. C.; McFarland, E. W.; Poojary, D. M.; Reaves, C. M.; Weinberg, W. H.; Wu, X. D. *Science* **1998**, *279*, 837.
(6) Wang, J.; Yoo, Y.; Gao, C.; Takeuchi, I.; Sun, X.; Chang, H.; Xiang, X.-D.; Schultz, P. G. *Science* **1998**, *279*, 1712.
(7) Reddington, E.; Sapienza, A.; Gurau, B.; Viswanathan, R.; Sarangapani, S.; Smotkin, E. S.; Mallouk, T. E. *Science* **1998**, *280*, 1735.
(8) (a) Senkan, S. M. *Nature* **1998**, *394*, 350. (b) Senkan, S. *Angew. Chem.* **2001**, *113*, 322; *Angew. Chem. Int. Ed. Engl.* **2001**, *40*, 312. (c) Senkan, S.; Ozturk, S *Angew. Chem.* **1999**, *111*, 867; *Angew. Chem., Int. Ed.* **1999**, *38*, 791.
(9) Jandeleit, B.; Schaefer, D. J.; Powers, T. S.; Turner, H. W.; Weinberg, W. H. *Angew. Chem.* **1999**, *111*, 2648; *Angew. Chem. Int. Ed.* **1999**, *38*, 2494.
(10) Guram, A.; Hagemeyer, A.; Lugmair, C. G.; Turner, H. W.; Volpe, A. F., Jr.; Weinberg, W. H.; Yaccato, K. *Adv. Synth. Catal.* **2004**, *346*, 215.
(11) (a) Klein, J.; Lehmann, C. W.; Schmidt, H. W.; Maier, W. F. *Angew. Chem.* **1998**, *110*, 3557. (b) Klein, J.; Lehmann, C. W.; Schmidt, H. W.; Maier, W. F. *Angew. Chem. Int. Ed.* **1998**, *37*, 3369.
(12) Baker, B. E.; Kline, N. J.; Treado, P. J; Natan, M. J. *J. Am. Chem. Soc.* **1996**, *118*, 8721.
(13) Pirrung, M. C. *Chem. Rev.* **1997**, *97*, 473.
(14) Maier, W. F.; Stowe, K.; Sieg, S. *Angew. Chem.* **2007**, *119*, 6122; *Angew. Chem. Int. Ed.* **2007**, *46*, 6016.
(15) Potyrailo, R. A.; Mirsky, V. M. *Chem. Rev.* **2008**, *108*, 770.
(16) Takeuchi, I.; Lauterbach, J.; Fasolka, M. J. *Mater. Today* **2005**, *8*, 18.
(17) Holland, J. H. In *Adaption in Natural and Artificial System*; University of Michigan Press *:* Ann Arbor, MI, 1975.
(18) Goldberg, D. E. In *Genetic Algorithm in Search, Optimization, and Machine Learning*; Addison-Wesley: Reading, MA, 1989.
(19) Forrest, S. *Science* **1993**, *261*, 872.
(20) Singh, J.; Ator, M. A.; Jaeger, E. P.; Allen, M. P.; Whipple, D. A.; Solowij, J. E.; Chowdhary, S.; Treasurywala, A. H. *J. Am. Chem. Soc.* **1996**, *118*, 1669.
(21) (a) Wolf, D.; Buyevskaya, V. O.; Baerns, M. *Appl. Catal., A* **2000**, *200*, 63. (b) Rodemerck, U.; Baerns, M.; Holena, M.; Wolf, D. *Appl. Surf. Sci.* **2004**, *223*, 168.
(22) Klanner, C.; Farrusseng, D.; Baumes, L.; Lengliz, M.; Mirodatos, C.; Schuth, F *Angew. Chem.* **2004**, *116*, 5461; *Angew. Chem. Int. Ed.* **2004**, *43*, 5347.
(23) Pereira, S. R. M.; Clerc, F.; Farrusseng, D.; Vander waal, J. C.; Mashmeyer, T. *QSAR Comb. Sci.* **2005**, *24*, 45.
(24) Serra, J. M.; Corma, A.; Valero, S.; Argente, E.; Botti, V. *QSAR Comb. Sci.* **2007**, *26*, 11.
(25) Breuer, C.; Lucas, M.; Schutze, F.-W.; Claus, P. *Comb. Chem. High Throughput Screening* **2007**, *10*, 59.
(26) Bulut, M.; Gevers, L. E. M.; Paul, J. S.; Vankelecom, I. F. J.; Jacobs, P. A. *J. Comb. Chem.* **2006**, *8*, 168.
(27) Greeley, J.; Jaramillo, T. F.; Bonde, J.; Chorkendorff, I. B.; Norskov, J. K. *Nat. Mater.* **2006**, *5*, 909.
(28) Falcioni, M.; Deem, M. W. *Phys. Rev. E* **2000**, *61*, 5948.
(29) (a) Sohn, K. -S.; Lee, J. M.; Shin, N. *Adv. Mater.* **2003**, *15*, 2081. (b) Sohn, K.-S.; Zeon, I. W.; Chang, H.; Lee, S. K.; Park, H. D. *Chem. Mater.* **2002**, *14*, 2140. (c) Sohn, K.-S.; Park, D. H.; Cho, S. H.; Kim, B. I. *J. Comb. Chem.* **2006**, *8*, 44.
(30) Jung, Y. S.; Kulshreshtha, C.; Kim, J. S.; Shin, N.; Sohn, K.-S. *Chem. Mater.* **2007**, *19*, 5309.
(31) Jansen, M. *Angew. Chem.* **2002**, *114*, 3896; *Angew. Chem. Int. Ed.* **2002**, *41*, 3746.
(32) Zitzler, E.; Thiele, L. *IEEE Trans. Evol. Comput.* **1999**, *3*, 257.
(33) Coello, C. A. C. *Knowledge Inf. Syst.* **1999**, *1*, 269.
(34) (a) Fonseca, C. M.; Fleming, P. J. *Evol. Comput.* **1995**, *3*, 1. (b) Fonseca, C. M; Fleming, P. J. In *Proceedings of the Fifth International Conference*; Morgan Kaufmann: San Mateo, CA, 1993; Vol. 416.
(35) (a) Horn, J.; Nalpliotis, N.; Goldberg, D. E. In *The Proceedings of the First IEEE Conference on Evolutionary Computation (ICEC 94)*; IEEE Service Center: Piscataway, NJ, 1994; Vol. 82.
(36) (a) Srinivas, N.; Deb, K. *Intl. J. Evol. Comput.* **1994**, *2*, 221. (b) Deb, K.; Goldberg, D. E. In *Proceedings of the Third International Conference on Genetic Algorithms*; Morgan Kaufmann: San Mateo, CA, 1991; Vol. 42.
(37) Deb, K.; Pratap, A.; Agrawal, S.; Meyarivan, T. *IEEE Trans. Evol. Comput.* **2002**, *6*, 182.
(38) Kalyanmoy, D. In *Multi-Objective Optimization using Evolutionary Algorithms*; John Willy & Sons: West Sussex, U.K., 2001.
(39) Coello, C.; Veldhuizen, D. V.; Lamont, G. *Evolutionary Algorithms for Solving Multiobjective Problems*; Kluwer Academic: New York, 2002.
(40) Kulshreshtha, C.; Sharma, A. K.; Sohn, K.-S. *J. Comb. Chem.* **2008**, *10*, 421.
(41) Kemeny, G.; Haake, C. H. *J. Chem. Phys.* **1960**, *33*, 783.

(42) Von Dreele, R. B.; Bless, P. W.; Kostiner, E.; Hughes, R. E. *J. Solid State Chem.* **1970**, *2*, 612.
(43) Williams, F. E. *J. Opt. Soc. Am.* **1949**, *37*, 302.
(44) Sarver, J. F.; Hummel, F. A. *J. Electrochem. Soc.* **1963**, *110*, 726.
(45) Iwasaki, M.; Kim, D. N.; Tanaka, K.; Murata, T.; Morinaga, K. *Sci. Technol. Adv. Mater.* **2003**, *4*, 137.
(46) Patten, S. H.; Williams, F. E. *J. Opt. Soc. Am.* **1949**, *39*, 702.
(47) Thorington, L. *J. Opt. Soc. Am.* **1950**, *40*, 579.

CC800116Q